

See discussions, stats, and author profiles for this publication at: <https://www.researchgate.net/publication/231667528>

Free-Standing Layer-By-Layer Hybrid Thin Film of Graphene-MnO₂ Nanotube as Anode for Lithium Ion Batteries

ARTICLE *in* JOURNAL OF PHYSICAL CHEMISTRY LETTERS · JULY 2011

Impact Factor: 7.46 · DOI: 10.1021/jz200836h

CITATIONS

112

READS

135

6 AUTHORS, INCLUDING:



Hey Woong Park

University of Waterloo

19 PUBLICATIONS 315 CITATIONS

SEE PROFILE



Drew C Higgins

University of Waterloo

70 PUBLICATIONS 2,083 CITATIONS

SEE PROFILE



Zhongwei Chen

University of Waterloo

179 PUBLICATIONS 5,221 CITATIONS

SEE PROFILE



Xingcheng Xiao

General Motors Company

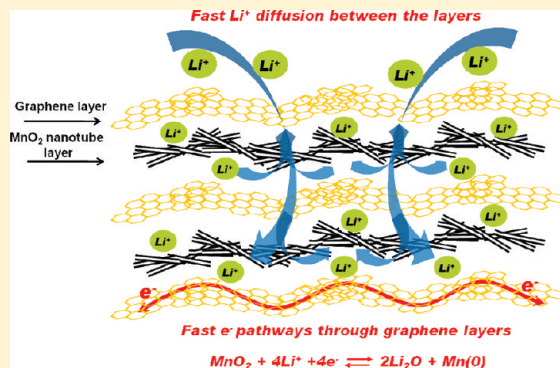
175 PUBLICATIONS 2,628 CITATIONS

SEE PROFILE

Free-Standing Layer-By-Layer Hybrid Thin Film of Graphene-MnO₂ Nanotube as Anode for Lithium Ion BatteriesAiping Yu,[†] Hey Woong Park,[†] Aaron Davies,[†] Drew C Higgins, Zhongwei Chen,^{*,†} and Xingcheng Xiao^{*,†}[†]Department of Chemical Engineering, University of Waterloo, 200 University Avenue West, Waterloo, Ontario, Canada N2L 3G1^{*}General Motors Global Research & Development Center, 30500 Mound Road, Warren, Michigan 48090, United States

ABSTRACT: Free-standing layer-by-layer assembled hybrid graphene-MnO₂ nanotube (NT) thin films were prepared by an ultrafiltration technique and studied as anodes for lithium ion batteries. Each thin layer of graphene provides not only conductive pathways accelerating a conversion reaction of MnO₂ but also buffer layers to maintain electrical contact with MnO₂ NT during lithium insertion/extraction. In addition, the unique structures of the thin film provide porous structures that enhance Li ion diffusion into the structure. The graphene-MnO₂ NT films as anode present excellent cycle and rate capabilities with a reversible specific capacity based on electrode composite mass of 495 mAh/g at 100 mA/g after 40 cycles with various current rates from 100 to 1600 mA/g. On the contrary, graphene-free MnO₂ NT electrodes demonstrate only 140 mAh/g at 80 mA/g after 10 cycles. Furthermore, at a high current rate of 1600 mA/g, the charge capacity of graphene-MnO₂ NT film reached 208 mAh/g.

SECTION: Energy Conversion and Storage



Lithium (Li) ion batteries are the most developed energy storage technology for various applications such as portable electronic devices, electric vehicles, and sustainable energy generation systems because of their attractive high gravimetric and volumetric energy densities compared with other energy storage technologies. However, since the initial commercial introduction of Li ion batteries composed of LiCoO₂ and graphite as cathode and anode materials, respectively, in the early 1990s by Sony, development of lithium ion batteries has fallen behind the rise in demand for safer, higher energy density and longer life cycle batteries. A variety of transition-metal oxide nanoparticles (NPs) have attracted great attention owing to their high theoretical electrochemical capacities.^{1–10} Poizot et al.¹ first introduced the concept of utilizing nanosized transition-metal oxides (MO, where M is Co, Ni, Cu or Fe) for Li ion battery applications because they were suggested to have even higher theoretical capacities than graphite because of their unique conversion reactions. However, large volume expansion during Li insertion/extraction destabilizes the structure of the MO and leads to a decrease in electrical contact between the current collector and active metal oxide, resulting in poor cyclability and rate capabilities.² Although diverse approaches, including the development of carbon-based composites with unique nano- and microstructures have been investigated in an attempt to overcome these drawbacks,^{3–10} ample opportunity remains to improve substantially the cell cycle and rate capabilities of electrode materials for use in Li ion batteries.

Graphene has also attracted significant attention in recent years because of its extraordinary electrical conductivity (as high

as 2200 S/m, depending on synthesis methods),¹¹ high surface areas of >2600 m²/g, chemical stability, and a distinct 2-D nanostructure. Because of the unique properties of graphene, it has been extensively investigated in the fabrication of free-standing, thin film materials because of recent technological trends focusing on flexible and portable devices.^{12,13} Moreover, graphene has been proposed to provide exemplary theoretical capacities of 1116 mAh/g,^{14,15} three times higher than commercial graphite, with its application demonstrated in high-capacity Li-ion battery assemblies.¹⁶ Graphene as a conductive matrix has also been applied to Co₃O₄,¹⁷ Fe₃O₄,¹⁸ and Mn₃O₄¹⁹ nanocomposites, which demonstrated superior performance as anode materials for Li ion batteries compared with previously reported results. Specifically, these combined transition-metal/graphene nanocomposites achieved high rate capabilities and reversible capacities with good cycle performance due to the addition of flexible graphene layers. The graphene layers were noted to provide a highly conductive structure in conjunction with a large surface area to support good contact between the MO NPs. In addition, graphene was effective in enhancing and maintaining the mechanical strength of the nanocomposite during volume changes as well as suppressing the aggregation of NPs during Li ion insertion/extraction.

In the present study, novel free-standing layer-by-layer (LBL) assembled graphene-MnO₂ nanotube (NT) thin film composites

Received: June 20, 2011

Accepted: July 11, 2011

Published: July 11, 2011

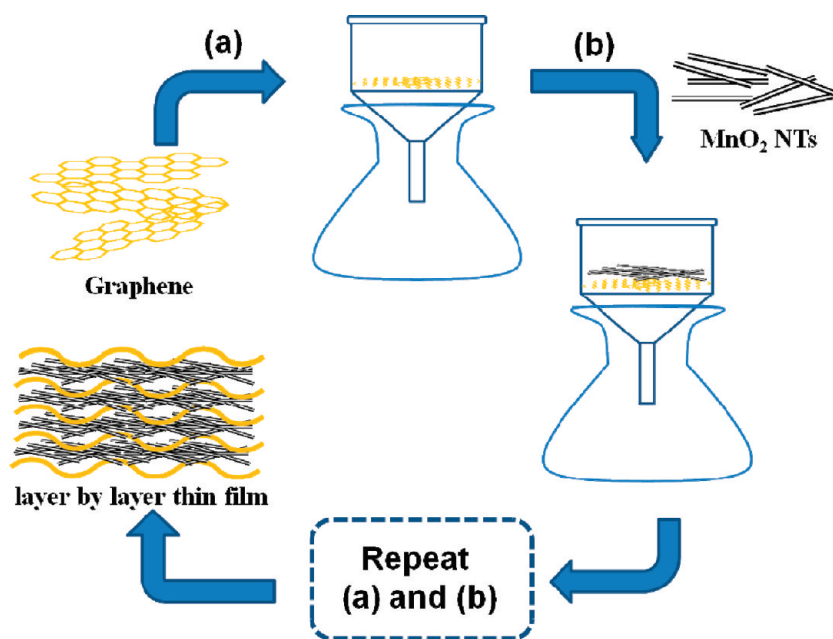


Figure 1. Schematic view for constructing (a) graphene and (b) MnO_2 layer-by-layer thin films on substrate.

were developed for use as anode materials in Li ion batteries. Numerous transition-metal oxides have been investigated for use as Li ion anode materials. In the present study, MnO_2 was selected because of the attractive economic and performance benefits. Specifically, Mn is very abundant and inexpensive, along with being environmentally friendly. Moreover, MnO_2 is recognized to have a high theoretical capacity (1232 mAh/g) based on heterogeneous Li_2O and Mn metal conversion reactions.^{7,20} The free-standing, graphene- MnO_2 nanocomposite film was assembled by a unique LBL assembly method, providing numerous advantages as Li ion anode materials, including: (1) During the formation of a LBL graphene- MnO_2 NT thin film, MnO_2 NT will hinder the restacking and ordering of graphene, allowing for a more porous structure to enhance Li ion diffusion during battery operation. (2) Graphene is in adequate contact with all MnO_2 NT providing a fast electron pathway with 2-D electron-conducting behavior between the MnO_2 NT. (3) The nanostructured thin film ($\sim 10\ \mu\text{m}$) shortens the diffusion path length for fast lithium ion transport into the electrode to enhance directly the power rating of the external circuit. (4) The mechanical and electrical properties of both graphene and MnO_2 NT enable the formation of strong, flexible electrodes, free of both binder and conducting additives. Each of these factors favor excellent electrochemical performance, and this graphene- MnO_2 nanocomposite thin film was demonstrated to have exemplary rate and cycle capabilities, with performance superior to pure MnO_2 NT as anode materials in Li ion batteries.

Using as-prepared graphene and MnO_2 NT, the novel LBL thin film was fabricated by an ultrafiltration method as described through a schematic representation (Figure 1). X-ray diffraction (XRD) patterns displayed in Figure 2 show characteristic graphene patterns with a broad (002) diffraction peak at $\sim 24^\circ$ corresponding to the average d -spacing of graphene layers. Confirmation of the crystal structure of as-prepared MnO_2 NT is also clearly shown, where all of the diffraction peaks observed indicate a α - MnO_2 phase.²¹ Additionally, the diffraction peaks for the LBL assembled graphene- MnO_2 thin film nanocomposite

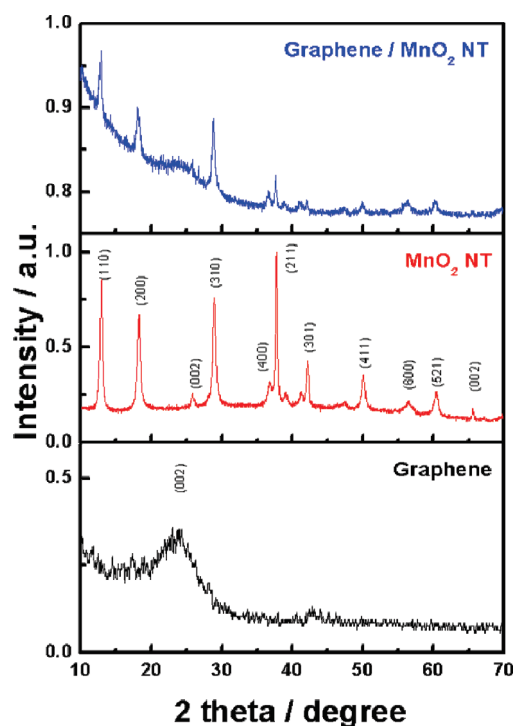


Figure 2. X-ray diffraction patterns of the graphene, MnO_2 NT, and LBL graphene- MnO_2 thin film.

correspond to individual graphene and MnO_2 NT indices, indicating that the structure of the individual materials is maintained following the fabrication of the LBL film.

Figure 3a presents a transmission electron microscopy (TEM) image of the wavy and wrinkled graphene sheets used for the formation of the free-standing films. Figure 3b shows a representative atomic force microscopy (AFM) image of graphene sheets in tapping mode (with a Nanoscope III, Digital Instruments).

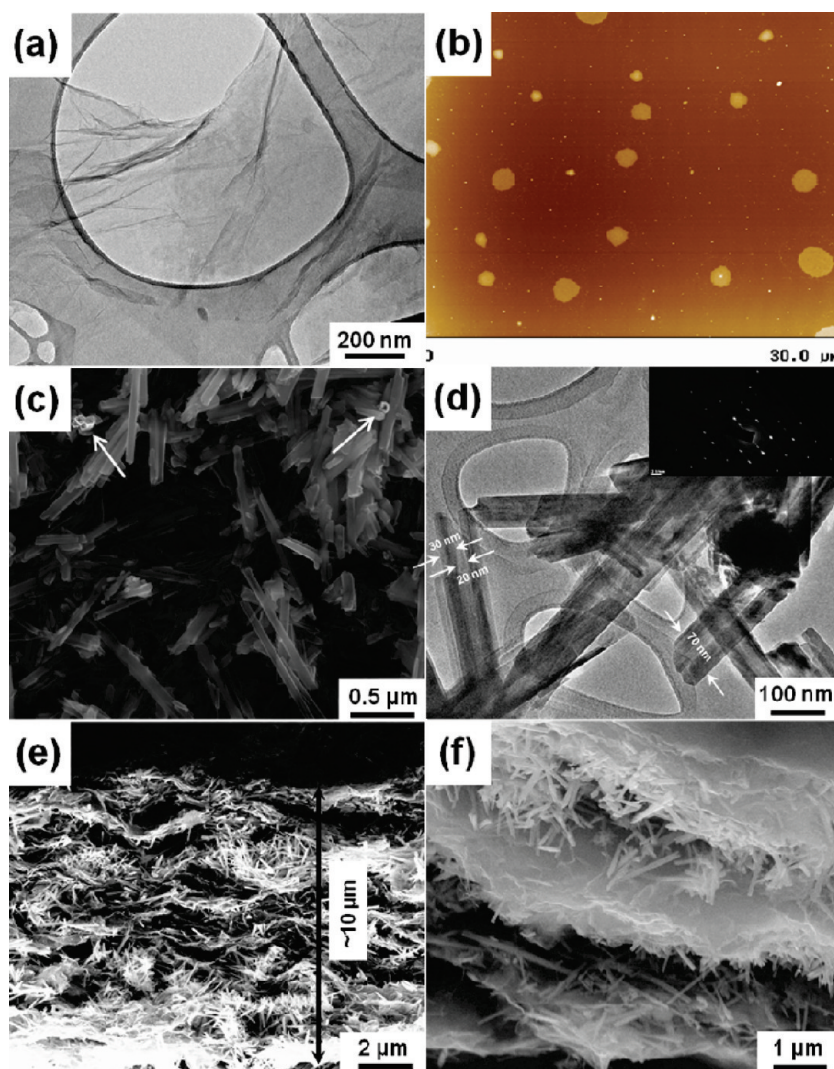


Figure 3. TEM and AFM images of (a,b) graphene; SEM and TEM images of (c,d) MnO₂ NT with different magnifications (inset: SAED pattern); and cross-sectional SEM images of (e,f) LBL graphene-MnO₂ NT thin film.

It was found that an average thickness of 1 to 2 nm was achieved for graphene sheets, which led to the conclusion that nearly complete exfoliation of graphene sheets down to a few layers was successful. The AFM image also shows that the size of the graphene sheets is comparable to those manually peeled off from pyrolytic graphite. The morphologies of the synthesized MnO₂ NT are shown by scanning electron microscopy (SEM) in Figure 3c. The synthesized MnO₂ NT having lengths of ca. 1 μm is shown to have a hollow structure with rectangular open ends clearly visible in Figure 3c, with diameters ranging from 70 to 80 nm. Figure 3d shows a TEM image where the wall thickness of the NTs is observed to be ~30 nm. An inset of the selected area electron diffraction (SAED) patterns of the same MnO₂ NT demonstrates the single-crystalline nature of the synthesized MnO₂ NT. SAED is consistent with results from a previous report attributing the growth of MnO₂ NT along the [001] direction (*c* axis).²¹

Cross-sectional investigations for the LBL structures were carried out by SEM, as shown in Figure 3e,f. The cross-sectional images of the LBL films in Figure 3e show deposited MnO₂ NT interspersed between layers of graphene, with an overall thickness

of ca. 10 μm. Certain graphene layers are difficult to distinguish as a result of the length of MnO₂ NTs disrupting layer continuity. It is proposed that the layered structure of the thin film can facilitate ion movement and reduce charge transfer resistance between the graphene layers. Moreover, the separated graphene layers can significantly enhance the overall electrical conductivity of the thin film due to the good contact with the MnO₂ and can serve to maintain the stable, rigid electrode structure displayed in Figure 3f during processing and battery operation.

Figure 4 shows the galvanostatic charge and discharge curves for (a) the LBL free-standing graphene-MnO₂ NT film and (b) the MnO₂ NT powder with carbon black and polyvinylidene fluoride (PVdF) in a weight ratio of 80:10:10 coated on a Cu current collector. The charge and discharge curves of the LBL graphene-MnO₂ film at a current density of 100 mA/g (based on electrode mass) demonstrated large irreversible capacities. This was caused by (i) the irreversible reactions of residual oxygen groups remaining on graphene during chemical reduction, (ii) the irreversible conversion reaction of the MnO₂ NT by Li ions, and (iii) the formation of a solid-electrolyte interface (SEI) layer by electrolyte decomposition (Figure 4a).^{8,9,13} The voltage plateau, found

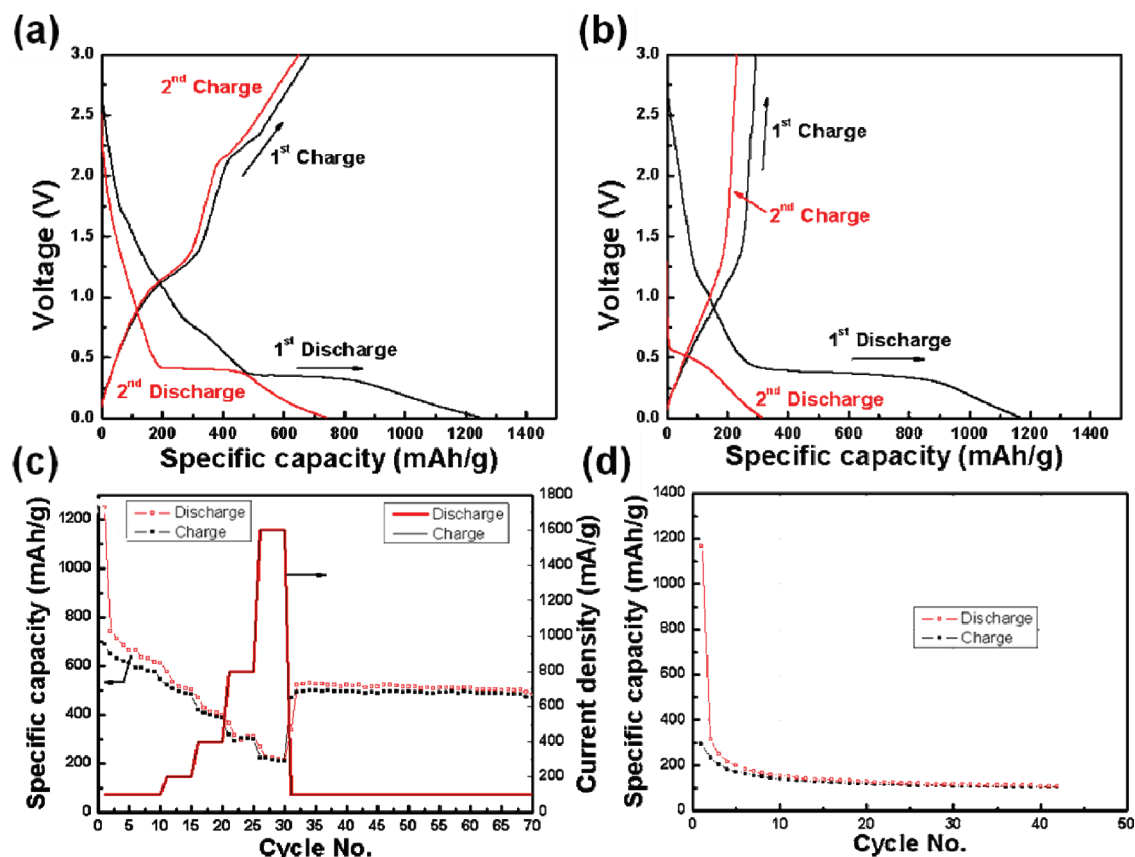


Figure 4. Galvanostatic charge and discharge curves of (a) LBL graphene-MnO₂ NT film, (b) graphene-free MnO₂ NT, (c) capacity of LBL graphene-MnO₂ NT film at various current rates from 100 to 1600 mA/g with respect to the cycle number, and (d) capacity of graphene-free MnO₂ NT at current rate of 80 mA/g with respect to the cycle number.

at 0.35 to 0.40 V, verified the transition-metal oxide conversion reactions of MnO₂ NT with Li ions, which is $\text{MnO}_2 + 4\text{Li}^+ + 4\text{e}^- \rightarrow \text{Mn}(0) + 2\text{Li}_2\text{O}$.²⁰ The charge curve, reflecting a reversible capacity up to ca. 2.15 V appears to be affected by the conversion reactions based on the charge curve of graphene-free MnO₂ NT electrode in Figure 4b, whereas the reversible capacity beyond 2.15 V is attributed to graphene. Furthermore, an acute decline of the irreversible capacity on the second cycle suggested the formation of an SEI layer during the initial cycle. Following the development of an SEI, an increase in the charge–discharge Coulombic efficiency is observed, representing the ratio of charge to discharge capacity. The initial irreversible capacities achieved for the LBL free-standing graphene-MnO₂ NT film and graphene-free MnO₂ NT electrodes were 581 and 873 mAh/g at the current rate of 100 and 80 mA/g, respectively (based on the total mass of electrodes except the current collector). These values demonstrate that the host graphene matrix enhances the reversibility of the transition-metal oxide redox reaction, with highly conductive graphene layers enabling the reduced form of the MnO₂ NT to participate in the oxidation reaction with Li ions. This effect results in the reversible capacity for the LBL free-standing graphene-MnO₂ NT film to reach 686 mAh/g. The capacity is lower than theoretical values of MnO₂ and graphene, which are 1232 and 1116 mAh/g, respectively; however, the capacity is much higher than that of graphene-free MnO₂ NT electrode (294 mAh/g in Figure 4b) as well as nearly twice that achieved by conventional graphite (~360 mAh/g).²² It

demonstrates that interspaced graphene layers (ca. 500 nm) can serve to facilitate electron transport to the MnO₂ NTs, along with their separation allowing ample room for Li ion diffusion into the electrode structure.²³ Figure 4c presents the results of current rate and cycle testing. After several cycles, fairly stable capacities for LBL free-standing graphene-MnO₂ NT film are observed, even at high current rates of 1600 mA/g. The 2-D electron conduction of graphene not only imparts high electron transport properties but also maintains the structure of MnO₂ NT layers within the film. Additionally, the unique LBL structure of the film can potentially improve Li ion mass diffusion into active sites of the structure and prevent graphene from restacking in the film. These effects are shown to improve the rate capability and cycle stability of the film. Moreover, the excellent rate capability is caused by the thickness of the thin films (~10 μm), which provides a smaller diffusion distance for lithium ions from the electrolyte to travel to an active site in the film and improves electron transport to an external circuit and notably also prevents damage of the electrode by large volume change of MnO₂ NT, improving the electrode stability.²⁴ As a result, the charge capacity of the LBL graphene-MnO₂ film with a current rate of 1600 mA/g to be 208 mAh/g (shown in Figure 4c), which is significantly better than conventional graphite recently reported having a capacity of 10–15 mAh/g achieved.²² Contrary to the results of the LBL thin film, which presents the capacity of 495 mAh/g at 100 mA/g after 40 cycles, Figure 4d demonstrates that the capacity of graphene-free MnO₂ NT electrode is stabilized

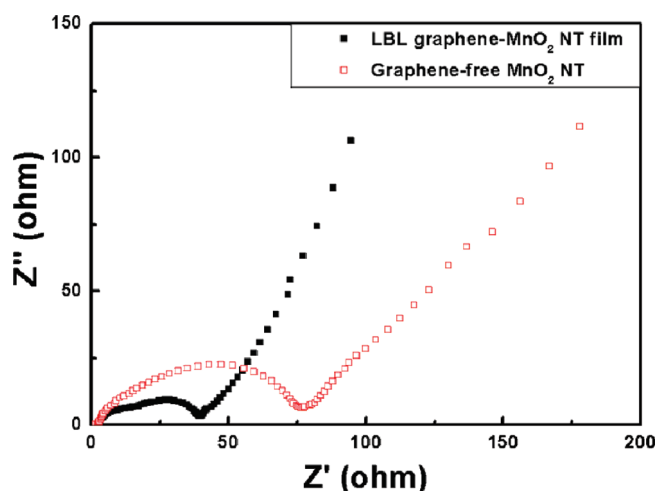


Figure 5. EIS results of the LBL graphene-MnO₂ NT film and graphene-free MnO₂ NT at fully discharged states.

around 140 mAh/g with a current rate of 80 mA/g after 10 cycles. The decrease in capacity is likely due to the loss of electrical contact between the particles caused by the large volume change during Li ion insertion/extraction. It indicates that the graphene layers play a role of conductive buffer layers to maintain electrical contacts with MnO₂ NT after the large volume change.

As shown in the rate capability test (Figure 4c), it is proposed that the unique LBL structure provides fast Li ion transportation in the thin film and accelerates the charge transfer reaction between the graphene layers and MnO₂ NT layers with migrated Li ions. This proposal is a critical factor to improve rate capability and is confirmed by electrochemical impedance spectroscopy (EIS) measurement compared with graphene-free MnO₂ NT electrode at fully discharged states (Figure 5). The results of EIS verify that charge transfer resistance of LBL graphene-MnO₂ film is much lower (~ 36 ohm) than that of graphene-free MnO₂ NT electrode. In other words, it is confirmed the charge transfer reactions in the LBL graphene-MnO₂ film are faster, improving the overall rate performance.

In conclusion, an ultrathin, free-standing and LBL assembled graphene-MnO₂ NT film with a unique nanostructure was prepared as an anode material for Li ion batteries. We propose that the unique film structures enhance Li ion diffusion to the active sites of the film, in addition to enhancement of the electrical conductivity by the large surface area graphene layers. Consequently, the composite film demonstrated not only 686 mAh/g of reversible capacity at a current rate of 100 mA/g, which is higher than achieved values from conventional graphite, but also 208 mAh/g at a high current rate of 1600 mA/g. Furthermore, the capacity became stabilized at ~ 500 mAh/g after cycling with various current rates. With the exceptional rate and cycle capabilities, free-standing LBL thin graphene-MnO₂ films are presented as promising anode materials for Li ion batteries.

EXPERIMENTAL METHODS

Graphene was produced by the reduction of graphene oxide prepared by a modified Hummer's method and has been described in detail elsewhere.²⁵ MnO₂ NT were synthesized by a hydrothermal reaction using KMnO₄ and has also been described in detail elsewhere.²¹ Stock solutions of dispersed graphene and MnO₂-NT with concentrations of 0.2 mg/mL

were prepared for film assembly. Composite films were assembled LBL, with each layer prepared by ultrafiltration of 1.2 mL stock solution thoroughly mixed by sonication in 250 mL of deionized (DI) water. By this method, the number of layers and composition of each were properly controlled. Following filtration of a 20-layer film (10 layers graphene, 10 layers MnO₂ NT, and the composition of the graphene/MnO₂ NT nanocomposites is 1:1 (weight ratio)) using a 0.2 μ m pore size alumina membrane (Whatman), the thin-film/membrane was air-dried and placed in DI water, where it became easily detached by floatation. The electrochemical performances were carried out using coin-type cells at the voltage range of 0.01 to 3.00 V, with Li metal as the counter and reference electrode and 1 M LiPF₆ in 3:7 ethylene carbonate (EC) and dimethyl carbonate (DMC) as the electrolyte. Various current densities at the voltage range of 0.01–3.00 V (vs Li metal) were applied for galvanostatic Li insertion/extraction tests. The EIS was conducted from a 1 MHz to 10 mHz frequency range with a 5 mV amplitude.

AUTHOR INFORMATION

Corresponding Author

*Tel: +1 519 888 4567, ext. 38664. Fax: +1 519 746 4979. E-mail: zhwchen@uwaterloo.ca; xingcheng.xiao@gm.com.

ACKNOWLEDGMENT

The University of Waterloo and the Natural Sciences and Engineering Research Council of Canada (NSERC) are gratefully acknowledged for their financial support for this work.

REFERENCES

- (1) Poizot, P.; Laruelle, S.; Grugeon, S.; Dupont, L.; Tarascon, J. M. Nano-Sized Transition-Metal Oxides as Negative-Electrode Materials for Lithium-Ion Batteries. *Nature* **2000**, *407*, 496–499.
- (2) Yao, W. L.; Yang, J.; Wang, J. L.; Tao, L. A. Synthesis and Electrochemical Performance of Carbon Nanofiber-Cobalt Oxide Composites. *Electrochim. Acta* **2008**, *53*, 7326–7330.
- (3) Yao, W. L.; Wang, J. L.; Yang, J.; Du, G. D. Novel Carbon Nanofiber-Cobalt Oxide Composites for Lithium Storage with Large Capacity and High Reversibility. *J. Power Sources* **2008**, *176*, 369–372.
- (4) Varghese, B.; Reddy, M. V.; Yanwu, Z.; Lit, C. S.; Hoong, T. C.; Rao, G. V. S.; Chowdari, B. V. R.; Wee, A. T. S.; Lim, C. T.; Sow, C. H. Fabrication of NiO Nanowall Electrodes for High Performance Lithium Ion Battery. *Chem. Mater.* **2008**, *20*, 3360–3367.
- (5) Zhang, H. J.; Tao, H. H.; Jiang, Y.; Jiao, Z.; Wu, M. H.; Zhao, B. Ordered CoO/CMK-3 Nanocomposites as the Anode Materials for Lithium-Ion Batteries. *J. Power Sources* **2010**, *195*, 2950–2955.
- (6) Cheng, M. Y.; Hwang, B. J. Mesoporous Carbon-Encapsulated NiO Nanocomposite Negative Electrode Materials for High-Rate Li-Ion Battery. *J. Power Sources* **2010**, *195*, 4977–4983.
- (7) Sun, B.; Chen, Z. X.; Kim, H. S.; Ahn, H.; Wang, G. X. MnO/C Core-Shell Nanorods as High Capacity Anode Materials for Lithium-Ion Batteries. *J. Power Sources* **2011**, *196*, 3346–3349.
- (8) Zhao, J. Z.; Tao, Z. L.; Liang, J.; Chen, J. Facile Synthesis of Nanoporous Gamma-MnO₂ Structures and their Application in Rechargeable Li-Ion Batteries. *Cryst. Growth Des.* **2008**, *8*, 2799–2805.
- (9) Zhong, K. F.; Xia, X.; Zhang, B.; Li, H.; Wang, Z. X.; Chen, L. Q. MnO Powder as Anode Active Materials for Lithium Ion Batteries. *J. Power Sources* **2010**, *195*, 3300–3308.
- (10) Shim, H. W.; Jin, Y. H.; Seo, S. D.; Lee, S. H.; Kim, D. W. Highly Reversible Lithium Storage in Bacillus Subtilis-Directed Porous Co₃O₄ Nanostructures. *ACS Nano* **2011**, *5*, 443–449.
- (11) Zhu, Y. W.; Stoller, M. D.; Cai, W. W.; Velamakanni, A.; Piner, R. D.; Chen, D.; Ruoff, R. S. Exfoliation of Graphite Oxide in Propylene

Carbonate and Thermal Reduction of the Resulting Graphene Oxide Platelets. *ACS Nano* **2010**, *4*, 1227–1233.

(12) Wang, C. Y.; Li, D.; Too, C. O.; Wallace, G. G. Electrochemical Properties of Graphene Paper Electrodes Used in Lithium Batteries. *Chem. Mater.* **2009**, *21*, 2604–2606.

(13) Abouimrane, A.; Compton, O. C.; Amine, K.; Nguyen, S. T. Non-Annealed Graphene Paper as a Binder-Free Anode for Lithium-Ion Batteries. *J. Phys. Chem. C* **2010**, *114*, 12800–12804.

(14) Pan, D. Y.; Wang, S.; Zhao, B.; Wu, M. H.; Zhang, H. J.; Wang, Y.; Jiao, Z. Li Storage Properties of Disordered Graphene Nanosheets. *Chem. Mater.* **2009**, *21*, 3136–3142.

(15) Li, X.; Geng, D.; Zhang, Y.; Meng, X.; Li, R.; Sun, X. Superior Cycle Stability of Nitrogen-Doped Graphene Nanosheets as Anodes for Lithium Ion Batteries. *Electrochem. Commun.* **2011**, doi: 10.1016/j.elecom.2011.05.012

(16) Lian, P. C.; Zhu, X. F.; Liang, S. Z.; Li, Z.; Yang, W. S.; Wang, H. H. Large Reversible Capacity of High Quality Graphene Sheets as an Anode Material for Lithium-Ion Batteries. *Electrochim. Acta* **2010**, *55*, 3909–3914.

(17) Wu, Z. S.; Ren, W. C.; Wen, L.; Gao, L. B.; Zhao, J. P.; Chen, Z. P.; Zhou, G. M.; Li, F.; Cheng, H. M. Graphene Anchored with Co_3O_4 Nanoparticles as Anode of Lithium Ion Batteries with Enhanced Reversible Capacity and Cyclic Performance. *ACS Nano* **2010**, *4*, 3187–3194.

(18) Zhou, G. M.; Wang, D. W.; Li, F.; Zhang, L. L.; Li, N.; Wu, Z. S.; Wen, L.; Lu, G. Q.; Cheng, H. M. Graphene-Wrapped Fe_3O_4 Anode Material with Improved Reversible Capacity and Cyclic Stability for Lithium Ion Batteries. *Chem. Mater.* **2010**, *22*, 5306–5313.

(19) Wang, H. L.; Cui, L. F.; Yang, Y. A.; Casalongue, H. S.; Robinson, J. T.; Liang, Y. Y.; Cui, Y.; Dai, H. J. Mn_3O_4 -Graphene Hybrid as a High-Capacity Anode Material for Lithium Ion Batteries. *J. Am. Chem. Soc.* **2010**, *132*, 13978–13980.

(20) Wu, M. S.; Chiang, P. C. J.; Lee, J. T.; Lin, J. C. Synthesis of Manganese Oxide Electrodes with Interconnected Nanowire Structure as an Anode Material for Rechargeable Lithium Ion Batteries. *J. Phys. Chem. B* **2005**, *109*, 23279–23284.

(21) Xiao, W.; Wang, D. L.; Lou, X. W. Shape-Controlled Synthesis of MnO_2 Nanostructures with Enhanced Electrocatalytic Activity for Oxygen Reduction. *J. Phys. Chem. C* **2010**, *114*, 1694–1700.

(22) Courtel, F. M.; Niketic, S.; Duguay, D.; Abu-Lebdeh, Y.; Davidson, I. J. Water-Soluble Binders for MCMC Carbon Anodes for Lithium-Ion Batteries. *J. Power Sources* **2011**, *196*, 2128–2134.

(23) Yoo, E.; Kim, J.; Hosono, E.; Zhou, H.; Kudo, T.; Honma, I. Large Reversible Li Storage of Graphene Nanosheet Families for Use in Rechargeable Lithium Ion Batteries. *Nano Lett.* **2008**, *8*, 2277–2282.

(24) Li, J. C.; Dozier, A. K.; Li, Y. C.; Yang, F. Q.; Cheng, Y. T. Crack Pattern Formation in Thin Film Lithium-Ion Battery Electrodes. *J. Electrochem. Soc.* **2011**, *158*, A689–A694.

(25) Yu, A. P.; Roes, I.; Davies, A.; Chen, Z. W. Ultrathin, Transparent, and Flexible Graphene Films for Supercapacitor Application. *Appl. Phys. Lett.* **2010**, *96*, 253105–253108.